Veterinary Immunology and Immunopathology 213 (2019) 109880

Contents lists available at ScienceDirect

Veterinary Immunology and Immunopathology

journal homepage: www.elsevier.com/locate/vetimm

Research paper

Changes in the intestinal mucosal proteome of turkeys (*Meleagris gallopavo*) infected with haemorrhagic enteritis virus

Andreia Tomás Marques[a], Sandra I. Anjo[b,c], Mangesh Bhide[d], Ana Varela Coelho[e], Bruno Manadas[b], Cristina Lecchi[a], Guido Grilli[a], Fabrizio Ceciliani[a,*]

[a] Università degli Studi di Milano, Department of Veterinary Medicine, Via Celoria 10, 20133, Milano, Italy
[b] CNC - Center for Neuroscience and Cell Biology, University of Coimbra, Rua Larga, Faculdade de Medicina, Pólo I, 1° andar, 3004-504, Coimbra, Portugal
[c] Faculty of Sciences and Technology, University of Coimbra, Universidade de Coimbra - Pólo II, Rua Sílvio Lima, 3030-790, Coimbra, Portugal
[d] Laboratory of Biomedical Microbiology and Immunology, University of Veterinary Medicine and Pharmacy, Komenskeho 73 Kosice, Slovakia
[e] Instituto de Tecnologia Química e Biológica António Xavier, Universidade Nova de Lisboa, Av. da República, 2780-157, Oeiras, Portugal

ARTICLE INFO

Keywords:
Haemorrhagic enteritis virus
Intestine
SWATH-MS
Meleagris gallopavo
Proteomics

ABSTRACT

Haemorrhagic enteritis (HE) is a viral disease affecting intestinal integrity and barrier function in turkey (*Meleagris gallopavo*) and resulting in a significant economic loss. Sequential Windowed Acquisition of All Theoretical Fragment Ion Mass Spectra (SWATH-MS) was applied to identify crucial proteins involved in HE infection. A total of 938 proteins were identified and used to generate a reference library for SWATH-MS analysis. In total, 523 proteins were reliably quantified, and 64 proteins were found to be differentially expressed, including 49 up-regulated and 15 down-regulated proteins between healthy and HE-affected intestinal mucosa. Functional analysis suggested that these proteins were involved in the following categories of cellular pathways and metabolisms: 1) energy pathways; 2) intestine lipid and amino acid metabolism; 3) oxidative stress; 4) intestinal immune response. Major findings of this study demonstrated that natural HE infection is related to the changes in abundance of several proteins involved in cell-intrinsic immune defense against viral invasion, systemic inflammation, modulation of excessive inflammation, B and T cell development and function and antigen presentation. mRNA quantitative expression demonstrated that most of the proteins involved in innate immunity that were found to be differentially abundant were produced by intestinal mucosa, suggesting its direct involvement in immune defences against HE infection.

1. Introduction

Haemorrhagic enteritis (HE) is an enteric disease affecting avian species, in particular turkeys (*Meleagris gallopavo*) older than 4 weeks of age, and compromising animal health and welfare. Haemorrhagic enteritis infection is regarded as one of the most important causes of economic loss to turkey industry. The mortality related to this disease ranges between 10–15% but it can reach 60% in some flocks (Dhama et al., 2017). The etiologic agent is the haemorrhagic enteritis virus (HE), a member of the family *Adenoviridae* type II (Suresh and Sharma, 1995). HE disease is characterized by acute onset of depression, pallor of the mucosae, splenomegaly, diarrhea, intestinal hemorrhage and sudden death. At day 5 after infection, haemorrhagic lesions and bleeding in the intestine start to occur. Very low levels of virus are detected in the intestinal tissue, even in the presence of intestinal lesions (Rautenschlein et al., 1998; Suresh and Sharma, 1996). Gross pathology description includes dilated intestine with blood content, and yellowish substance on the intestinal mucosa (Dhama et al., 2017). Severe congestion in the intestinal mucosa, degeneration, shortening of the villi and bleeding at the tips of them are identified at microscopic level (Sharma, 1991). Surviving birds are immunodepressed as a consequence of the lymphotrophic and lymphocytopathic attitude of the virus, which facilitates secondary infections with opportunistic pathogens agents such as the avian pathogenic *Escherichia coli*, bacterial respiratory diseases or septicemia (Koncicki et al., 2012; Moura-Alvarez et al., 2014).

Although HE has been known since 1937 (Pomeroy and Fenstermacher, 1937), the molecular mechanisms of viral immunopathogenesis and immunosuppression are mostly unknown. No information about how the virus infection modifies the intestinal proteome is available as well.

To date, proteomic studies in poultry gastrointestinal tract are

* Corresponding author.
E-mail address: fabrizio.ceciliani@unimi.it (F. Ceciliani).

https://doi.org/10.1016/j.vetimm.2019.06.001
Received 5 February 2019; Received in revised form 4 June 2019; Accepted 7 June 2019

limited to chicken (*Gallus gallus*) (Luo et al., 2013; Matulova et al., 2013; O'Reilly and Eckersall, 2014; Zhang et al., 2015). To the best of our knowledge, no proteomic data about intestine protein asset is available in turkey.

In order to elucidate the molecular mechanisms underlying the pathogenesis related to HE infection, we performed a quantitative evaluation of the proteome changes of the intestinal mucosa in turkeys after HE acute infection as compared with healthy mucosa by applying a Sequential Windowed Acquisition of All Theoretical Fragment Ion Mass Spectra (SWATH-MS) strategy. The mRNA quantification of genes related to proteins involved in immune recognition was also determined, in order to assess the effective capability of intestinal mucosa to produce the proteins that were differentially abundant.

2. Materials and methods

2.1. Samples collection and preservation

The present study was carried out on commercial B.U.T. BIG6 hybrid turkeys. Four clinically healthy turkeys were randomly selected during routine slaughtering procedures from 80 day-old females as previously described (D'Andreano et al., 2017). Pathological analysis of the gastroenteric tract evidenced no sign of gross pathological lesions related to enteritis. Molecular diagnosis to rule out the presence of HEV was carried out in the 4 tracts of intestine and spleen by means of specific PCR (Hess et al., 1999). A second group of four turkeys PCR HE positive (HE-infected animals) was included. This group of animals showed evident acute clinical signs of HE, and were subjected to euthanasia due to their critical clinical conditions, by cervical dislocation. Portions of jejunum, where the lesions were observed, were removed immediately after euthanasia: the mucosa was scratched, snap frozen into liquid nitrogen and afterwards stored at − 80 °C.

2.2. Protein extraction and digestion

Protein extraction of jejunal mucosa was carried out on ice, following a general protocol for lysis of cells in 2.5 fold lysis buffer. In short, 400 mg of each tissue was washed with cold phosphate buffer saline (PBS), traces of blood were removed and tissue was homogenized in 1 ml lysis buffer (50 mM Tris pH 7.4, 150 mM NaCl, 1% Triton X-100, 1% IGEPAL, 0. 1% SDS) with 10 µl Protease Inhibitor Cocktail (Sigma-Aldrich). Tissue disruption was performed using a tissue homogenizer (Precellys 24, Bertin Technologies) (4 cycles, 5500 rpm, 20 s) and glass beads (0.1 mm, Bertin Technologies) and sonicated on ice (10 cycles, 10 s). Protein extracts were centrifuged for 10 min, 10, 000 x g at 4 °C. Protein concentration was determined using the method of Bradford (1976) and the absorbance was measured at 700 nm using Odyssey® CLx Infrared Imaging System (LI − COR, Biosciences).

Protein extracts were hydrolyzed in-solution, essentially as previously described (Llombart et al., 2016). Samples were adjusted to a concentration of 2 µg/µL with 6 M Urea and 50 mM NH_4HCO_3 pH = 8.5. Two µg of green fluorescence protein fused with maltose binding protein (MBP-GFP) was used as internal standard for each sample. Samples were digested with trypsin **Gold** (Promega) (trypsin:protein = 1:20, w/w) for 18 h at 37 °C. Each sample was completely dried and then re-suspended in 100 µl of 2% acetonitrile (ACN) with 1% formic acid (FA) and sonicated in the ultrasound bath for 5 min with low amplitude. The digested peptides were de-salted and concentrated using C18 Bond Elut OMIX solid phase extraction pipette tips (Agilent Technologies) as previously described (Silva et al., 2016). Peptides were then eluted with 100 µL of 70% ACN with 0.1% FA and, after evaporation, the pellets were stored at –20 °C.

2.3. SWATH acquisition

Peptides were resuspended in 50 µL of a solution of 2% ACN and 0. 1% FA, and 10 µL of each sample were used to create two pooled samples. Four biological samples per condition were used to create the pooled samples for protein identification (four healthy animals and four HE-positive animals). In order to remove insoluble material, the peptide mixtures were then centrifuged for 5 min at 14,000 × g and collected into the proper vial for LC–MS analysis.

Samples were analysed on a Triple TOF™ 5600 System (ABSciex®) in two phases: information-dependent acquisition (IDA) of the pooled samples and, SWATH acquisition of each individual sample. Peptides were resolved by liquid chromatography (nanoLC Ultra 2D, Eksigent®) on a MicroLC column ChromXP™ C18CL (300 µm ID × 15 cm length, 3 µm particles, 120 Å pore size, Eksigent®) at 5 µL/min with a multistep gradient: 0–2 min linear gradient from 2 to 5%, 2–45 min linear gradient from 5% to 30% and, 45–46 min to 35% of ACN in 0.1% FA and 5% dimethyl sulfoxide (DMSO). Peptides were eluted into the mass spectrometer using an electrospray ionization source (DuoSpray™ Source, ABSciex®) with a 50 µm internal diameter (ID) stainless steel emitter (NewObjective).

The information dependent acquisition (IDA) experiments were performed for each pooled sample in a total of two acquisitions per pool. The mass spectrometer was set to scanning full spectra (350–1250 m/z) for 250 ms, followed by up to 100 MS/MS scans (100–1500 *m/z* from a dynamic accumulation time – minimum 30 ms for precursor above the intensity threshold of 1000 – in order to maintain a cycle time of 3. 3 s). Candidate ions with a charge state between +2 and +5 and counts above a minimum threshold of 10 counts per second were isolated for fragmentation and one MS/MS spectrum was collected before adding those ions to the exclusion list for 25 s (mass spectrometer operated by Analyst® TF 1.7, ABSciex®). Rolling collision was used with a collision energy spread of 5.

For SWATH-MS based experiments, the mass spectrometer was operated in a looped product ion mode (Gillet et al., 2012) and the same chromatographic conditions used as in the IDA run described above. A set of 60 windows (Supplementary Table 1) of variable width (containing 1 *m/z* for the window overlap) was constructed covering the precursor *m/z* range of 350-1250. A 250 ms survey scan (*m/z* 350–1500) was acquired at the beginning of each cycle for instrument calibration and SWATH MS/MS spectra were collected from *m/z* 100–1500 for 50 ms resulting in a cycle time of 3.25 s from the precursors ranging from *m/z* 350 to 1250. The collision energy for each window was determined according to the calculation for a charge +2 ion centered upon the window with variable collision energy spread (CES) according with the window.

2.4. Database searches and quantification

A specific library of precursor masses and fragment ions was created by combining all files from the IDA experiments, and used for subsequent SWATH processing. The library was obtained using ProteinPilot™ software (v5.1, ABSciex®), using the following parameters: i) search against a database composed by all the entries for the species *Meleagris gallopavo* (https://www.ncbi.nlm.nih.gov/protein?LinkName= genome_protein&from_uid=112) which comprised 24,245 non-redundant sequences and *Gallus gallus* (https://www.ncbi.nlm.nih.gov/protein/?term=Gallus+gallus+genome) which comprised 53,468 non-redundant sequences from NCBI (April 2018), and the sequence of the recombinant MBP-GFP protein (IS); ii) iodoacetamide alkylated cysteines as fixed modification; and iii) trypsin as digestion type. An independent False Discovery Rate (FDR) analysis using the target-decoy approach provided with ProteinPilot™ software was used to assess the quality of the identifications and positive identifications were considered when identified proteins and peptides reached a 5% local FDR (Sennels et al., 2009; Tang et al., 2008).

Data processing was performed using SWATH™ processing plug-in for PeakView™ (v2. 0. 01, ABSciex®) (Lambert et al., 2013). Peak group confidence threshold was determined based on a FDR analysis using the

target-decoy approach and 1% extraction FDR threshold was used for all the analyses. Peptide that met the 1% FDR threshold in at least three of the four biological replicates were retained, and the peak areas of the target fragment ions of those peptides were extracted across the experiments using an extracted-ion chromatogram (XIC) window of 4 min with 100 ppm XIC width.

The levels of the proteins were estimated by summing all the transitions from all the peptides for a given protein that met the criteria described above, as adapted from (Collins et al., 2013) and normalized to the total intensity of each sample. The internal standard (MBP-GFP) was used to performed retention time alignment.

2.5. Functional annotation and grouping

The retrieved protein FASTA sequences were loaded on the open source online tool Blast2GO 4. 0. 2 software (http://www.blast2go.com). The default parameters were used and, for the basic local alignment search tool (BLAST), protein sequences were mapped against the NCBI database. The functional analysis was further narrowed by PANTHER classification (http://www.pantherdb.org). WEGO (http://wego.genomics.org.cn) has used to build graphics. Kyoto encyclopedia of genes and genomes (KEGG) database (released on April 2018) was used to classify identified proteins into specific functional terms and metabolic pathways.

2.6. RT-qPCR

In order to elucidate the capability of intestinal jejunal mucosa to produce the mRNA of proteins identified by SWATH-MS, RT-qPCR of genes involved in immunity, inflammatory pathways and response to pathogens was carried out. Total RNA was extracted from the same samples using TriZol standard protocol (Invitrogen). The RNA concentration was quantified by use of the NanoDrop ND-1000 spectrophotometer (NanoDrop Technologies). The purity of RNA ($A_{260/A280}$) was ˜2. Genomic DNA was eliminated using DNase I (Invitrogen) and reverse transcription was performed with1μgRNA as the template, using the iSCRIPT cDNA Synthesis Kit (BioRad).

Primers were designed on turkey sequences available in NCBI by using Primer 3 (http://bioinfo.ut.ee/primer3-0.4.0), preventing possible secondary structures with the mfold Web Server (http://mfold.rna.albany.edu/?q=mfold/DNA-Folding-Form) and ensuring the specificity of the sequence by Clustal Omega (http://www.ebi.ac.uk/Tools/msa/clustalo). The primer sequences and fragment length are presented in Table 1.

Quantitative real time PCR (qPCR) was performed using 12 μL Eva Green Supermix (BioRad) using Eco Real-Time PCR System (Illumina). The concentration of primers is reported in Table 1. GAPDH, RPL4 and YWHAZ were selected as reference genes (Marques et al. (2016)). In order to assess the PCR efficiency using a relative standard curve, series of dilution were prepared by performing four-fold serial dilution starting from the pooled sample composed of a liver cDNA mix from four healthy animals. Each sample was tested in duplicate. Non-reverse transcribed controls were performed by omitting reverse transcription and no template controls were conducted by adding nuclease free water. The thermal profile used (95 °C for 10 min, 40 cycles of 95 °C for 10 s and 60 °C for 30 s; for melting curve construction, 55 °C for 15 s and 80 cycles starting to 55 °C and increasing 0.5 °C each for 10 s) was the same for each target gene. The MIQE guidelines were followed (Bustin et al., 2009). For all genes studied, the standard curves derived from serial dilution of pooled sample gave correlation coefficients (R^2) greater than 0. 990 and efficiencies greater than 94%. Results were compared using the comparative $^{\Delta-\Delta}$Cq method.

2.7. Statistical analysis

Data analysis was conducted with principal component analysis (PCA) and partial least squares discriminant analysis (PLS-DA) using SIMCA P software package (Umetrics) in order to observe intrinsic clusters and obvious outliers (based on the principles of Hotelling T^2) within the dataset. Statistical analysis was performed using XLSTAT for Windows (Addinsoft). Normality of data was checked by Shapiro–Wilk test. Data was compared by a Student t-test, with a two-tailed distribution and a homoscedastic variance for parametric data, while Wilcoxon signed rank test was applied in case of nonparametric data. Significance accepted for p-values ≤ 0.05.

3. Results

3.1. Protein identification, quantification by SWATH-MS and functional grouping of intestinal mucosa proteome

The aim of the present study was to investigate for the first time the effects of HE infection in jejunum on the proteome mapping of jejunal mucosa collected from 4 healthy and 4 HE-positive turkeys. Protein target database resources of turkey are still incomplete and poorly annotated. Therefore, aiming to increase the number of proteins that can be identified, turkey and chicken, composed by nonredundant proteins from NCBI database were combined.

Table 1
List of the genes under study and their respective primers sequences, accession numbers and fragment lengths.

Gene	GenBank	Primer Forward (5'–3')	Primer Reverse (5'–3')	Length (bp)	RT-qPCR concentration
PIT54	XM_003202017	GCCAGTGCAATTTGTTCAGA	TCCCGTAAATCCCAGTTGTC	146	100 nM
SELENBP1	XM_010724013.1	AACCTGAAAGACGAGCTCCA	AGATCAGGCATGGGAGAATG	103	200 nM
HPX	XM_010706282.1	CTTCCAGGGTGAGAAGGTCTG	CTCCTCAGGGTGACACTCCA	130	150 nM
CORO2A	XM_010726179.1	GTCCCTCGATGGTCAGAGTC	GTCCAGAGCCTGGTCTCAAG	139	N/A
FGB	XM_003205349.2	TCAGGCAGAGAATGTGAGGA	GGCTTGGTAAAAGGATCTGGC	86	200 nM
MPST	XM_010711524.1	CAAGCCAGATGTTGCTGTGT	TCCCAAATCCAGTTTCAAGG	156	300 nM
PGRMC1	NM_001271939.1	GAGGTCTTGCCACTTTCTGC	TTCAGCAGCTTACCAACGTG	148	250 nM
CANX	XM_003210435.2	ATGGAAACCCAGGAAGATCC	CACAGCACTGAAGGGAGTCA	79	100 nM
IGLL1	XM_010720331.1	ACACCAACAGACCCTCGAAC	CAGTGCTGCTGTCGTAGCTC	135	N/A
PPIA	NM_001166326.1	GTGCCCATAACAGCAGAGAAC	ACCACCCTGACACATGAAGC	111	100 nM
GPA33	XM_010721705.1	ATGACAGTCAGCGTTGTCCC	TTCTCTTGCCGTCTCCTCGT	150	N/A
CALM	NM_205005.1	ACTTGGTCAGAACCCCACAG	TCAATTGTGCCATTGCCATCAG	78	200 nM
GAPDH	GQ184819.1	GATCCCTTCATCGACCTGAA	ACAGTGCCCTTGAAGTGTCC	77	400 nM
RPL4	XM_003209573.1	TGTTTGCCCCAACCAAGACT	TCCTCAATGCGGTGACCTTT	136	400 nM
YWHAZ	XM_003205203.1	TTCCCTTGCAAAAACGGCTT	TTCAGCTTCGTCTCCTTGGG	148	400 nM

PIT54, scavenger receptor cysteine-rich domain-containing protein LOC284297 homolog (haptoglobin-like); SELENBP1, selenium-binding protein 1-A; HPX, hemopexin; CORO2A, coronin-2A; FGB, fibrinogen beta chain; MPST, 3-mercaptopyruvate sulfurtransferase; PGRMC1, membrane-associated progesterone receptor component; CANX, calnexin; IGLL1, immunoglobulin lambda-like polypeptide 1; PPIA, peptidyl-prolyl cis-trans isomerase A; GPA33, cell surface A33 antigen; CALM, calmodulin.

Using SWATH-MS strategy, a library was created with 7013 identified peptides, corresponding to 938 different proteins across both conditions (Supplementary Tables 2 and 3, respectively). After filtering for proteins which were quantified in at least three of four biological replicates and with at least one peptide (FDR ≤ 1% and a confidence of at least 99%), this library allowed the quantification of 523 proteins among the eight samples, which were included in this comparative and descriptive analysis (Supplementary Table 4).

From a dataset composed by 523 proteins, 185 protein number identifiers were successfully functionally assigned on UniProtKB website (http://www.uniprot.org) and 45 were mapped on PANTHER website. More than 60% of the UniProtKB proteins were lacking and/or were classified as "Uncharacterized protein"; therefore, we ran BLAST using Blast2GO software to annotate the protein dataset.

Gene Ontology (GO) analysis was performed using the three main ontologies (Cellular Component, Molecular Function and Biological Process). Blast2GO retrieved 841 unique Biological Process GO terms, 541 unique Molecular Function GO terms and 800 unique Cellular Component GO terms associated with the dataset. From 523 total proteins, 18 sequences were not annotated. Gene Ontology classification using WEGO (Web Gene Ontology) Annotation Plot (http://wego.genomics.org.cn) is presented in Fig. 1.

The 523 quantified proteins were grouped into 28 GO terms divide into the three main ontology classes: i) Cellular component – 40.6% cell, 23.4% macromolecular complex, 17.2% organelle part, 10.9% extracellular region, and 7.8% membrane-enclosed lumen; ii) Molecular function – 57.8% binding, 39.1% catalytic activity, 3.1% transporter activity; and iii) Biological process – 42.2% metabolic process, 42.2% cellular process, 6.3% localization, 4.7% pigmentation, 3.1% anatomical structure formation, and 1.6% response to stimulus.

3.2. Differential quantification and statistical analysis of intestinal mucosa proteins between HE and control groups

To identify differentially abundant proteins between the two studied conditions, statistical analysis was applied, and fold-changes and *p*-values were used to rank and filter the quantitative data (Fig. 2). Differentially abundant proteins were defined as those that showed a fold change with a *p*-value ≤0. 05. In total, 64 proteins differentially abundant between the healthy and HE groups were identified in the turkey intestine, which included 49 proteins up-regulated and 15 down-regulated proteins in HE-affected animals (Table 2). Following KEGG classification, the 64 differently abundant proteins were grouped into nine classes based on their putative functions: amino acid and protein metabolism (25%), carbohydrate metabolism (19%), fatty acids metabolism (16%), cytoskeleton (11%), immune system (11%), nucleic acid biogenesis (6%), ribosome (6%), binding and transport (5%) and apoptosis (1%), as shown in Fig. 3. Proteins related to amino acid and protein metabolism, carbohydrate metabolism, fatty acids metabolism, cytoskeleton and immune system were predominant and accounted for approximately 80% of the differential proteins.

The significant similarity of the 4 biological replicates samples and the noticeable differences of protein patterns between healthy and HE-infected intestine did not result in distinct segregation of the proteomes after PCA analysis applied to the 523 quantified proteins as multivariate statistical method. On the contrary, four healthy animals and four diseased animals show a clear separation into two groups after PLS-DA analysis (Fig. 4).

3.3. mRNA expression of selected proteins related with immune system

The intestine is crossed by a wide capillary network. The finding of a protein by proteomic techniques does not confirm its expression by intestine. Therefore, several proteins can be expressed by liver or other tissues and then delivered to intestine through blood. The effective ability of jejunal mucosa to produce proteins related with immune response was confirmed by RT-qPCR through detection of their respective mRNAs. We focused our attention on those differentially expressed proteins that were found to be up-regulated more than 2 times in healthy mucosa and involved in innate immunity and inflammatory response, namely selenium-binding protein 1-A (SELENBP1), hemopexin (HPX), PIT54, fibrinogen beta chain (FGB), membrane-associated progesterone receptor component (PGRMC1), immunoglobulin lambda-like polypeptide 1 (IGLL1) and cell surface A33 antigen (GPA33),

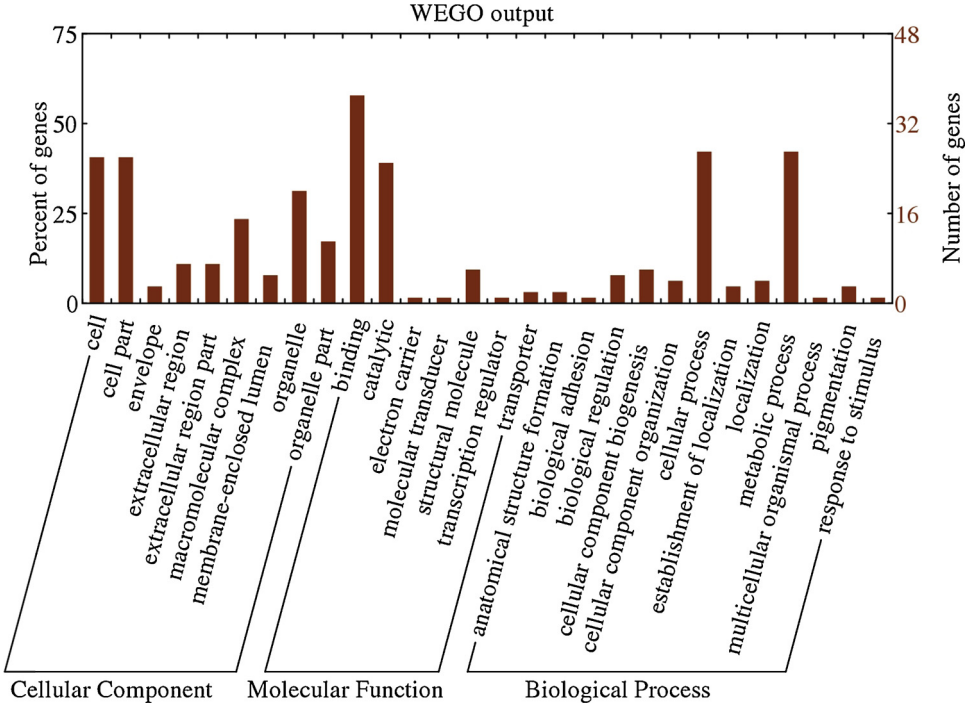

Fig. 1. Proteome characterization of mucosa intestine. GO classification using Blast2GO shows level 2 categories for Cellular Components, Molecular Function and Biological Processes.

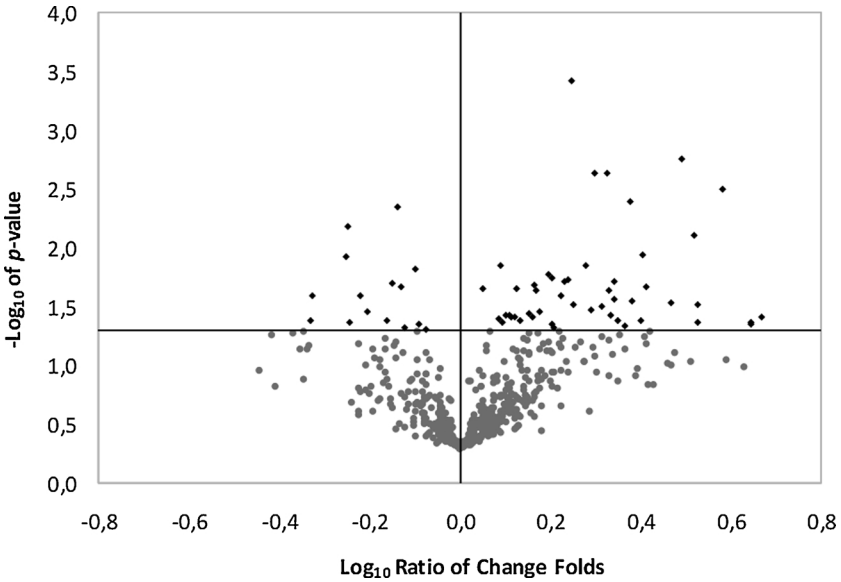

Fig. 2. The distribution of *p*-values and fold changes (log10) in 523 quantitative proteinsbetween the healthy and HE-infected groups. A total of 64 proteins were selected as different proteins, which exhibited a *p*-value ≤0. 05.

coronin-2A (CORO2A), 3-mercaptopyruvate sulfurtransferase (MPST), calnexin (CANX), peptidyl-prolyl cis-trans isomerase A (PPIA) and calmodulin (CALM), which are related to inflammation, viral and bacterial defenses and response to external stimulus.

The mRNA expression studies are presented in Fig. 5. Quantitative analysis confirmed that at least 6 of the proteins involved in immunity and inflammatory response were produced by jejunal mucosa, although the difference between healthy and HE infected animals was found not significant. mRNA coding for SELENBP1, PPIA, MPST, PGRMC1, CANX and CALM didn't show any statistical difference. Remarkably, the relative differences in abundancy between amount of the three acute phase proteins (APP) included in the list of differentially expressed proteins, namely FGB, PIT54 and HPX, is negligible in both healthy and infected mucosa.

4. Discussion

This study shows the differential changes in the intestinal proteome of turkey and how it is modified following the infection with HE. Although HE is regarded as one of the leading causes of viral intestinal diseases in turkeys, the molecular background of its pathogenesis and how the local immune system reacts to the invasion of the virus are mostly unknown. By using a next generation proteomic approach, the SWATH-MS, we described the jejunal mucosa proteomes of HE-infected turkeys as compared to healthy ones. The effective capability of jejunal mucosa to produce the proteins identified by means of proteomics analysis was further investigated by quantitative gene expression analysis.

The KEGG classification analysis revealed that out of 64 differentially abundant proteins in HE intestinal mucosa proteome, a number of 43 (66%) are involved in protein, carbohydrate, fatty acid and nucleic acid metabolism. This result is consistent with previous metabolic studies showing that viruses can induce modification in host cell metabolism, including an increase of glycolysis and fatty acid synthesis, increasing the amount of energy available for virus replication (Thai et al., 2014). Changes in nucleotide, amino acid and protein metabolism may provide an increase in pools of free aminoacids and nucleotides necessary to cope with viral genome replication and virus assembly (Sanchez and Lagunoff, 2015). A total of 11% of differentially abundant proteins were related to cytoskeleton, including, among the others, WD and Coronin1, which are decreased in intestinal mucosa from HEV affected turkeys. Coronins are essential regulators of Ca^{2+} trafficking after T cell receptor stimulation, and a decrease of Coronin1 has been linked to a $CD4^{+}$ T cell response during viral infection (Tchang et al., 2013).

The focus of the present work was to study the involvement of intestinal mucosa on immune defenses and inflammation against HE infection. We provided the evidence that natural HE infection is linked to the changes in abundance of proteins related to cell-intrinsic immune defense against viral invasion, systemic inflammation, modulation of excessive inflammation, B and T cell development and function and antigen presentation.

4.1. Proteins related to cell intrinsic immune defense against virus

HE infection induces a decrease in the abundance of DDX3X (DEAD-Box Helicase 3 X-Linked). Decreasing of DDX3X leads to a significant reduction of infectious HSV-1 particles (Khadivjam et al., 2017), suggesting the activation of a defensive mechanism in HE as well.

4.2. Proteins involved in systemic reaction to inflammation

As expected, HE infection prompted an inflammatory response as confirmed by the increased abundance of proteins related to systemic reaction to inflammation, such as FBG (fibrinogen β chain), PIT54 and HPX (Hemopexin) (O'Reilly and Eckersall, 2014; Adler et al., 2001; Ceciliani et al., 2002). The presence of FGB in turkey HE-intestine confirms previous studies in chicken infected with gastrointestinal diseases (Georgieva et al., 2010). The PIT54 is regarded as one of the major APP in poultry (O'Reilly and Eckersall, 2014) and is upregulated in turkeys stressed after road transport (Marques et al., 2016). PIT54 extrahepatic expression has been recently demonstrated in chicken, but its mRNA abundance in healthy animals was shown to be negligible (Marques et al., 2017). The increased abundance of FBG, PIT54 and HPX provides the evidence that HE infection triggers a local inflammatory reaction and, given the involvement of fibrinogen, the activation of a coagulation cascade. On the background that the increase of mRNA of FBG, PIT54 and HPX in intestinal mucosa of HE affected turkeys is negligible, we hypothesize that the local increase of APP is related to a translocation of proteins from blood serum to intestinal mucosa. These hypothesis is confirmed by previous finding (Takagi et al., 2012) that have also reported the presence of HPX protein in

Table 2
List of proteins differentially expressed in the intestinal mucosa in healthy and HE-affected intestine. Protein fold changes in HE-affected compared to healthy intestine are shown.

Accession	Name	Protein	Fold	*p*-value
gi|733885686	CASP6	PREDICTED: caspase-6 [Meleagris gallopavo]	4.63	0.0385
gi|733883237	DECR1	PREDICTED: 2, 4-dienoyl-CoA reductase, mitochondrial [Meleagris gallopavo]	4.41	0.0438
gi|475808004	SDHA	succinate dehydrogenase [ubiquinone] flavoprotein subunit, mitochondrial [Gallus gallus]	4.40	0.0427
gi|513231603	LOC427292	PREDICTED: S-adenosylmethionine synthase isoform type-2-like isoform X2 [Gallus gallus]	3.79	0.0031
gi|971417755	HSDL2	PREDICTED: heterogeneous nuclear ribonucleoprotein A/B isoform X2 [Gallus gallus]	3.36	0.0429
gi|733926850	HNRPAB	PREDICTED: hydroxysteroid dehydrogenase-like protein 2, partial [Meleagris gallopavo]	3.36	0.0298
gi|733929326	DHDH	PREDICTED: trans-1, 2-dihydrobenzene-1, 2-diol dehydrogenase [Meleagris gallopavo]	3.30	0.0078
gi|733921537	SELENBP1	PREDICTED: selenium-binding protein 1-A isoform X2 [Meleagris gallopavo]	3.09	0.0017
gi|971370598	HIST1H2B5L	PREDICTED: histone H2B 1/2/3/4/6-like [Gallus gallus]	2.94	0.0290
gi|733919423	PCYOX1	PREDICTED: prenylcysteine oxidase 1 [Meleagris gallopavo]	2.58	0.0216
gi|971378941	HPX	PREDICTED: hemopexin [Gallus gallus]	2.53	0.0114
gi|971384254	RPL7	PREDICTED: 60S ribosomal protein L7 isoform X1 [Gallus gallus]	2.52	0.0408
gi|733893517	RPL14	PREDICTED: 60S ribosomal protein L14 [Meleagris gallopavo]	2.40	0.0283
gi|733910438	ATP5J2	PREDICTED: ATP synthase subunit f, mitochondrial [Meleagris gallopavo]	2.38	0.0040
gi|326924446	ES1	PREDICTED: ES1 protein homolog, mitochondrial-like [Meleagris gallopavo]	2.30	0.0459
gi|733868906	PIT54	PREDICTED: soluble scavenger receptor cysteine-rich domain-containing protein SSC5D-like [Meleagris gallopavo]	2.23	0.0411
gi|71897175	COPA	coatomer subunit alpha [Gallus gallus]	2.19	0.0192
gi|733928504	LOC104915868	PREDICTED: pyruvate carboxylase, mitochondrial-like, partial [Meleagris gallopavo]	2.18	0.0275
gi|971392610	ETFDH	PREDICTED: electron transfer flavoprotein-ubiquinone oxidoreductase, mitochondrial isoform X2 [Gallus gallus]	2.16	0.0371
gi|733894380	HSPE1	PREDICTED: 10 kDa heat shock protein, mitochondrial [Meleagris gallopavo]	2.13	0.0232
gi|971375846	GK	PREDICTED: glycerol kinase isoform X4 [Gallus gallus]	2.11	0.0023
gi|733918251	RPL22	PREDICTED: 60S ribosomal protein L22, partial [Meleagris gallopavo]	2.06	0.0314
gi|50755667	NDUFB10	PREDICTED: NADH dehydrogenase [ubiquinone] 1 beta subcomplex subunit 10 [Gallus gallus]	1.99	0.0023
gi|733890971	PSMA3	PREDICTED: proteasome subunit alpha type-3 [Meleagris gallopavo]	1.95	0.0338
gi|733926972	CORO2A	PREDICTED: coronin-2A [Meleagris gallopavo]	1.89	0.0140
gi|487442401	SDHB	succinate dehydrogenase [ubiquinone] iron-sulfur subunit, mitochondrial isoform 2 precursor [Gallus gallus]	1.78	0.0297
gi|733884061	FGB	PREDICTED: fibrinogen beta chain [Meleagris gallopavo]	1.76	0.0004
gi|166091440	SRSF1	serine/arginine-rich splicing factor 1 [Gallus gallus]	1.73	0.0186
gi|971420700	SEPT2L	PREDICTED: septin-2 isoform X2 [Gallus gallus]	1.70	0.0192
gi|326922507	HSPD1	PREDICTED: 60 kDa heat shock protein, mitochondrial [Meleagris gallopavo]	1.67	0.0251
gi|971440071	HSD17B4	PREDICTED: peroxisomal multifunctional enzyme type 2 isoform X1 [Gallus gallus]	1.62	0.0468
gi|733870043	MPST	PREDICTED: 3-mercaptopyruvate sulfurtransferase isoform X2 [Meleagris gallopavo]	1.60	0.0448
gi|971437427	TLN1	PREDICTED: talin-1 isoform X3 [Gallus gallus]	1.60	0.0181
gi|429903872	PGRMC1	membrane-associated progesterone receptor component 1 [Gallus gallus]	1.57	0.0166
gi|733911356	UBE2L3	PREDICTED: ubiquitin-conjugating enzyme E2 L3 [Meleagris gallopavo]	1.50	0.0343
gi|733909243	CANX	PREDICTED: LOW QUALITY PROTEIN: calnexin [Meleagris gallopavo]	1.47	0.0229
gi|733881362	ECI2	PREDICTED: enoyl-CoA delta isomerase 2, mitochondrial isoform X1 [Meleagris gallopavo]	1.46	0.0205
gi|733925751	RPS6	PREDICTED: 40S ribosomal protein S6 [Meleagris gallopavo]	1.44	0.0388
gi|733912151	IGLL1	PREDICTED: immunoglobulin lambda-like polypeptide 1 isoform X2 [Meleagris gallopavo]	1.41	0.0362
gi|733921095	DLAT	PREDICTED: dihydrolipoyllysine-residue acetyltransferase component of pyruvate dehydrogenase complex, mitochondrial [Meleagris gallopavo]	1.36	0.0416
gi|261490820	PPIA	peptidyl-prolyl cis-trans isomerase A [Gallus gallus]	1.33	0.0218
gi|326919055	MTTP	PREDICTED: microsomal triglyceride transfer protein large subunit [Meleagris gallopavo]	1.32	0.0385
gi|733888683	CPT1A	PREDICTED: carnitine O-palmitoyltransferase 1, liver isoform [Meleagris gallopavo]	1.30	0.0386
gi|733872460	GPA33	PREDICTED: cell surface A33 antigen [Meleagris gallopavo]	1.29	0.0374
gi|971380110	HNRNPA2B1	PREDICTED: heterogeneous nuclear ribonucleoproteins A2/B1 isoform X5 [Gallus gallus]	1.26	0.0369
gi|45384366	CALM	calmodulin [Gallus gallus]	1.24	0.0432
gi|733897806	GOT1	PREDICTED: aspartate aminotransferase, cytoplasmic, partial [Meleagris gallopavo]	1.22	0.0140
gi|743405597	DDX4	probable ATP-dependent RNA helicase DDX4 [Gallus gallus]	1.22	0.0397
gi|733893848	LOC100547885	PREDICTED: UDP-glucuronosyltransferase 1-1-like isoform X5 [Meleagris gallopavo]	1.12	0.0217
gi|326928043	ACOX2	PREDICTED: peroxisomal acyl-coenzyme A oxidase 2 [Meleagris gallopavo]	−1.19	0.0492
gi|52138693	WDR1	WD repeat-containing protein 1 [Gallus gallus]	−1.23	0.0445
gi|482661640	CORO1C	coronin-1C isoform 1 [Gallus gallus]	−1.26	0.0150
gi|733870073	MYH9	PREDICTED: myosin-9 [Meleagris gallopavo]	−1.33	0.0471
gi|971431933	ATP5L	PREDICTED: ATP synthase subunit g, mitochondrial [Gallus gallus]	−1.36	0.0216
gi|971411979	TPM1	PREDICTED: tropomyosin alpha-1 chain isoform X16 [Gallus gallus]	−1.37	0.0044
gi|50746903	CISD2	PREDICTED: CDGSH iron-sulfur domain-containing protein 2 [Gallus gallus]	−1.41	0.0201
gi|733903686	SI	PREDICTED: sucrase-isomaltase, intestinal [Meleagris gallopavo]	−1.46	0.0418
gi|45382893	CALB1	calbindin [Gallus gallus]	−1.61	0.0344
gi|733873176	DDX3X	PREDICTED: ATP-dependent RNA helicase DDX3X [Meleagris gallopavo]	−1.67	0.0250
gi|733927467	LOC104915494	PREDICTED: fatty acyl-CoA hydrolase precursor, medium chain-like [Meleagris gallopavo]	−1.76	0.0429
gi|733905607	LOC104912905	PREDICTED: creatine kinase U-type, mitochondrial-like [Meleagris gallopavo]	−1.78	0.0065
gi|733922734	ACE	PREDICTED: LOW QUALITY PROTEIN: angiotensin-converting enzyme [Meleagris gallopavo]	−1.79	0.0117
gi|733912766	LOC100539678	PREDICTED: serine dehydratase-like [Meleagris gallopavo]	−2.12	0.0254
gi|326919083	BDH2	PREDICTED: 3-hydroxybutyrate dehydrogenase type 2 [Meleagris gallopavo]	−2.15	0.0409

injured intestinal mucosa of rats, but not at mRNA level.

4.3. Proteins involved in changes of B-cell and T-cell population

One of the major features of HE infection is turkey is a dramatic change of B-cell and T-cell population, which is depleted because of the viral infection ((Suresh and Sharma, 1996, Suresh and Sharma, 1995)). The proteomic results presented in this study partially provide a molecular background to these changes, demonstrating that HE infection is related to changes in the abundance of proteins involved in B-cells and T cells development and differentiation, such as IGLL1, PGRMC1, PPIA and CALM.

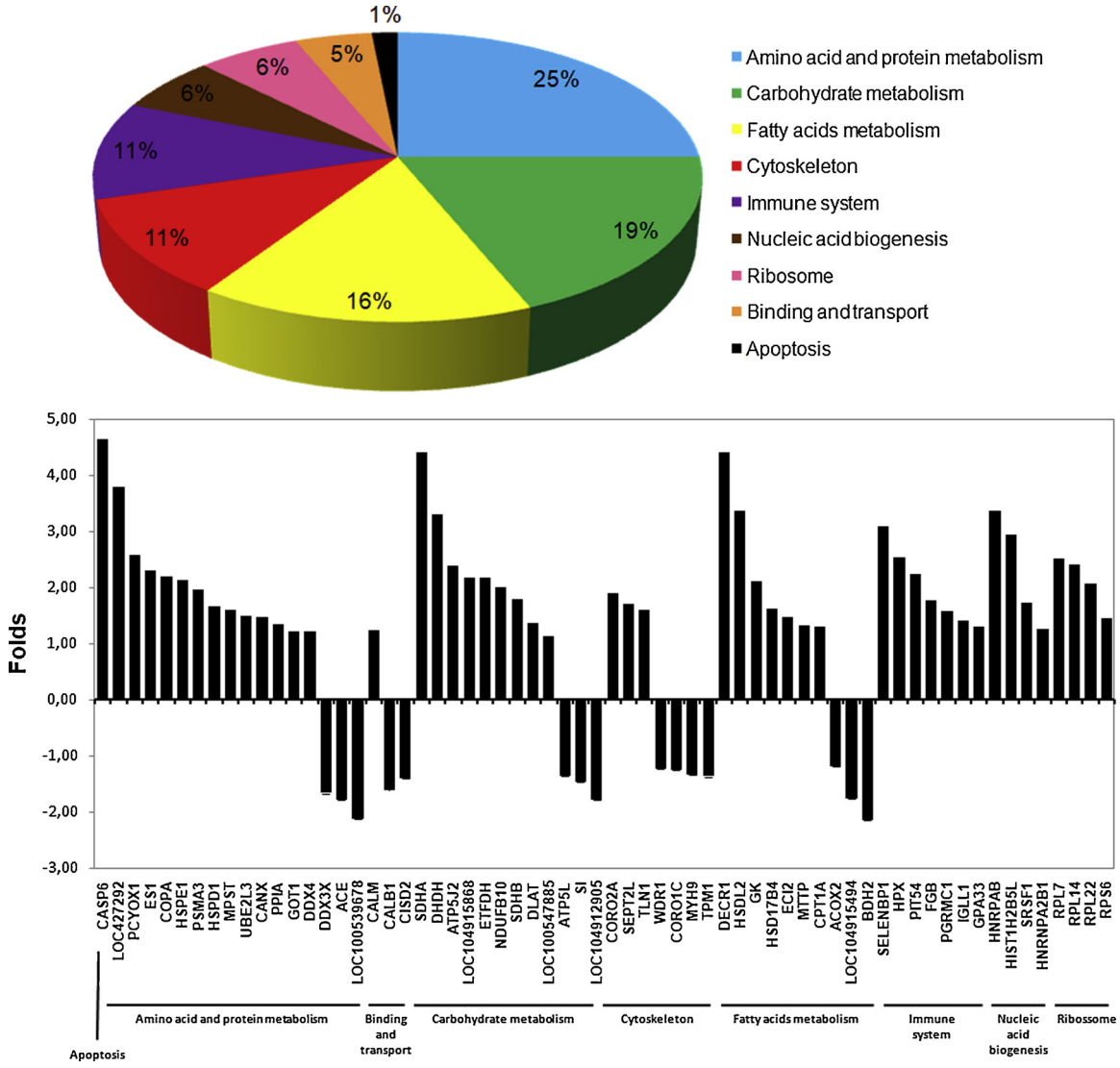

Fig. 3. Functional classification of the proteins of differential abundance identified from the intestinal mucosa of turkey.

The IGLL1 gene encodes a component of the pre-B-cell receptor, which is crucial for B cells development (Chen et al., 2016) and dysfunctions of the IGLL1 gene cause a primary immunodeficiency related to poorer proliferation and differentiation of pro-B cells and consequently, lower levels of serum antibodies and circulating B cells (Bankovich et al., 2007). PGRMC1 is a single transmembrane protein that forms part of a multi-protein complex that binds to progesterone and other steroids, and a recent report suggested that its expression is

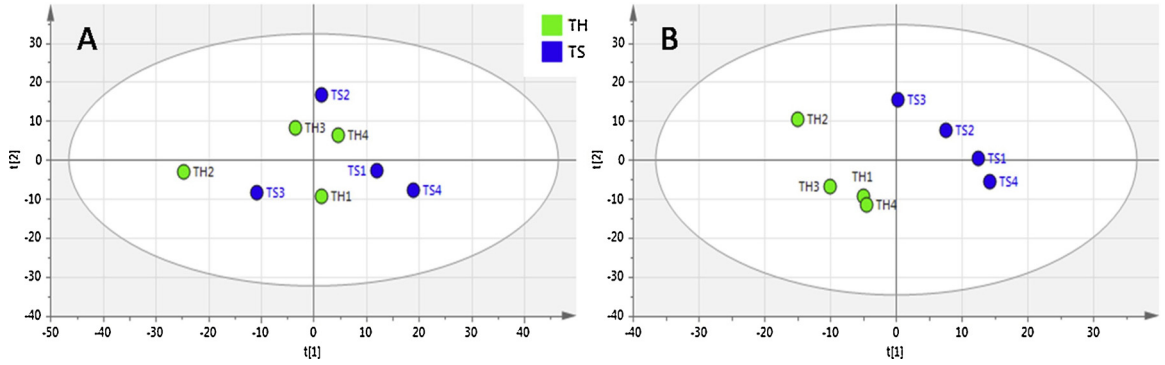

Fig. 4. PCA and PLS-DA score-plots from healthy and HE-affected groups. A: Score-plot obtained from PCA modelling, 2 components extracted. Healthy group, green. HE-infected group, blue. The first component explains 35% ($R^2X[1] = 0.345$) of the variation and the second component 17% ($R^2X[2] = 0.167$). B: Score-plot obtained from PLS-DA modelling, 2 components extracted. Healthy group, green. HE-infected group, blue. The first component explains 30% ($R^2X[1] = 0.269$) of the variation and the second component 20% ($R^2X[2] = 0.20$). (For interpretation of the references to colour in this figure legend, the reader is referred to the web version of this article).

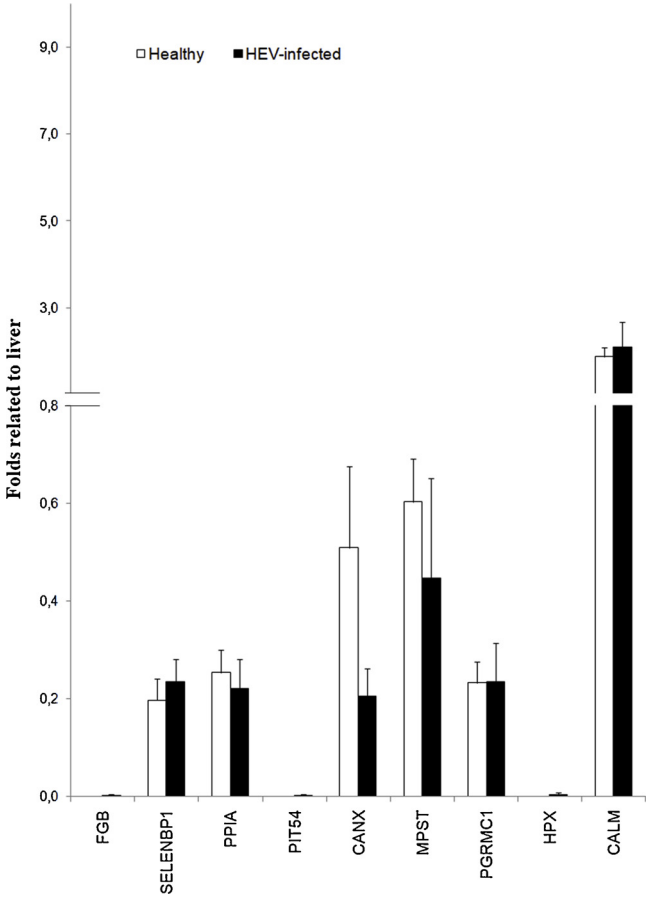

Fig. 5. Relative expression of PIT54, PGRMC1, SELENBP1, HPX, FGB, CANX, MPST, PPIA and CALM in liver and intestine of healthy and HE-infected turkeys studied by qPCR. The results were normalized using the geometric mean of reference genes (GAPDH, YWHAZ and RPL4). Data are means ± SEM of four animals. Folds relative to liver = 1.

involved in Th1/Th2 and Treg regulation (Maeda et al., 2013). PPIA (also known as Cyclophilin A) is associated with viral infections in chicken, such as Influenza Virus and Infectious Bursal Disease Virus (Frausto et al., 2013; Wang et al., 2015), and is involved in T cell activation and in the IFN-I or IL-2 responses during virus infections (Dawar et al., 2017). Finally, Calmodulin (CALM), which increased in HE infected intestinal cells, is involved in T cell apoptosis (Contini et al., 2005). The increase abundance of PRGM1, PPIA, CALM and IGLL1 in intestinal mucosa during HE suggests the activation of a local immune system and the reaction to the presence of the virus, as demonstrated by the local expression of mRNA coding for these proteins.

4.4. Proteins involved in modulating excessive immune response

The proteomic analysis carried out in this study also identified a significant increase of proteins whose role is to modulate excessive immune response, such as SELENBP1, COROA2 and MPST. SELENBP1 is a member of selenium-binding protein family, which has been shown to bind selenium covalently (Porat et al., 2000). The role of SELENBP1 in intestine is to modulate the differentiation and function of immune cells, contributing to reduce excessive immune response (Speckmann and Steinbrenner, 2014). COROA2 has been shown to fulfill an anti-inflammatory function, being required to de-repress TLR target genes by macrophages (Huang et al., 2011). Further protective effects against excessive inflammatory response may be provided by MPST (Mercaptopyruvate Sulfurtransferase), whose abundance is increase in HE affected animals and may provide an antioxidant activity (Nagahara et al., 2019).

4.5. Proteins involved in antigen presentation

The list of proteins whose abundance is modified due to HE infection in intestinal mucosa includes also proteins involved in antigen presentation, such as Calnexin (CANX) and GPA33. CANX is part of the chaperon machinery involved in antigen presentation and is also involved in intestinal Paneth cells' differentiation (Gassler et al., 2002; Huang et al., 2016). GPA33 is also involved in immune signaling and antigen presentation. GPA33 is an intestinal epithelium-specific cell surface marker and a component of the tight junction-associated proteins of the immunoglobulin superfamily (Ackerman et al., 2008). Beside its activity on antigen presentation, GPA33 is also crucial for the maintenance of intestinal barrier function (Williams et al., 2015). An increased abundance of GPA33 might be related to a protective function against excessive intestinal leakage.

5. Conclusions

This study presented the first proteomic comparison of healthy and HE-affected intestinal mucosa proteome in turkey, focusing on immune reaction against virus, and demonstrating that several proteins that were found to be differentially expressed are involved in several pathways related to immune defense against viruses. Our findings provide insight in the immunological pathways activated by HE infection, in particular for what concerns the different abundance of proteins involved in B and T cell regulation and development. Further work is necessary to establish the precise mechanism by which up-regulating or down-regulating of these proteins provide protection against the disease.

Acknowledgments

This work was financed by the European Regional Development Fund (ERDF) through the COMPETE 2020 - Operational Programme for Competitiveness and Internationalisation and Portuguese national funds via FCT – Fundação para a Ciência e a Tecnologia, I. P., under projects: POCI-01-0145-FEDER-007440 (ref. ; UID/NEU/04539/2013), POCI-01-0145-FEDER-016428 (ref. : SAICTPAC/0010/2015), and POCI-01-0145-FEDER-016795 (ref. : PTDC/NEU-SCC/7051/2014).

SIA was supported by PhD fellowship SFRH/BD/81495/2011 co-financed by the European Social Fund (ESF) through the POCH - Programa Operacional do Capital Humano and national funds via FCT. "

Appendix A. Supplementary data

Supplementary material related to this article can be found, in the online version, at doi:https://doi.org/10.1016/j.vetimm.2019.06.001.

References

Dhama, K., Gowthaman, V., Karthik, K., Tiwari, R., Sachan, S., Kumar, M.A., Palanivelu, M., Malik, Y.S., Singh, R.K., Munir, M., 2017. Haemorrhagic enteritis of turkeys - current knowledge. Vet. Q. 37, 31–42. https://doi.org/10.1080/01652176.2016.1277281.

Suresh, M., Sharma, J.M., 1995. Hemorrhagic enteritis virus induced changes in the lymphocyte subpopulations in turkeys and the effect of experimental immunodeficiency on viral pathogenesis. Vet. Immunol. Immunopathol. 45, 139–150.

Rautenschlein, S., Suresh, M., Neumann, U., Sharma, J.M., 1998. Comparative pathogenesis of haemorrhagic enteritis virus (HEV) infection in turkeys and chickens. J. Comp. Pathol. 119, 251–261.

Suresh, M., Sharma, J.M., 1996. Pathogenesis of type II avian adenovirus infection in turkeys: in vivo immune cell tropism and tissue distribution of the virus. J. Virol. 70, 30–36.

Sharma, J.M., 1991. Hemorrhagic enteritis of turkeys. Vet. Immunol. Immunopathol. 30, 67–71.

Koncicki, A., Tykałowski, B., Stenzel, T., Smiałek, M., Pestka, D., 2012. Effect of infection of turkeys with haemorrhagic enteritis adenovirus isolate on the selected parameters of cellular immunity and the course of colibacillosis. Pol. J. Vet. Sci. 15, 215–220.

Moura-Alvarez, J., Nuñez, L.F.N., Astolfi-Ferreira, C.S., Knöbl, T., Chacón, J.L., Moreno, A.M., Jones, R.C., Ferreira, A.J.P., 2014. Detection of enteric pathogens in Turkey flocks affected with severe enteritis, in Brazil. Trop. Anim. Health Prod. 46, 1051–1058. https://doi.org/10.1007/s11250-014-0612-7.

Pomeroy, B.S., Fenstermacher, R., 1937. Hemorrhagic enteritis in turkeys. Poult. Sci. 16, 378–382.

Luo, J., Zheng, A., Meng, K., Chang, W., Bai, Y., Li, K., Cai, H., Liu, G., Yao, B., 2013. Proteome changes in the intestinal mucosa of broiler (Gallus gallus) activated by probiotic Enterococcus faecium. J. Proteomics 91, 226–241. https://doi.org/10.1016/j.jprot.2013.07.017.

Matulova, M., Varmuzova, K., Sisak, F., Havlickova, H., Babak, V., Stejskal, K., Zdrahal, Z., Rychlik, I., 2013. Chicken innate immune response to oral infection with Salmonella enterica serovar Enteritidis. Vet. Res. 44, 37. https://doi.org/10.1186/1297-9716-44-37.

O'Reilly, E.L., Eckersall, P.D., 2014. Acute phase proteins: a review of their function, behaviour and measurement in chickens. Worlds Poult. Sci. J. 70, 27–44. https://doi.org/10.1017/S0043933914000038.

Zhang, J., Li, C., Tang, X., Lu, Q., Sa, R., Zhang, H., 2015. Proteome changes in the small intestinal mucosa of broilers (Gallus gallus) induced by high concentrations of atmospheric ammonia. Proteome Sci. 13, 9. https://doi.org/10.1186/s12953-015-0067-4.

D'Andreano, S., Sànchez Bonastre, A., Francino, O., Cuscó Martí, A., Lecchi, C., Grilli, G., Giovanardi, D., Ceciliani, F., 2017. Gastrointestinal microbial population of turkey (Meleagris gallopavo) affected by hemorrhagic enteritis virus. Poult. Sci. 96, 3550–3558. https://doi.org/10.3382/ps/pex139.

Hess, M., Raue, R., Hafez, H.M., 1999. PCR for specific detection of haemorrhagic enteritis virus of turkeys, an avian adenovirus. J. Virol. Methods 81, 199–203.

Llombart, V., García-Berrocoso, T., Bech-Serra, J.J., Simats, A., Bustamante, A., Giralt, D., Reverter-Branchat, G., Canals, F., Hernández-Guillamon, M., Montaner, J., 2016. Characterization of secretomes from a human blood brain barrier endothelial cells in-vitro model after ischemia by stable isotope labeling with aminoacids in cell culture (SILAC). J. Proteomics 133, 100–112. https://doi.org/10.1016/j.jprot.2015.12.011.

Silva, C., Santa, C., Anjo, S.I., Manadas, B., 2016. A reference library of peripheral blood mononuclear cells for SWATH-MS analysis. Proteomics Clin. Appl. 10, 760–764. https://doi.org/10.1002/prca.201600070.

Gillet, L.C., Navarro, P., Tate, S., Röst, H., Selevsek, N., Reiter, L., Bonner, R., Aebersold, R., 2012. Targeted data extraction of the MS/MS spectra generated by data-independent acquisition: a new concept for consistent and accurate proteome analysis. Mol. Cell Proteomics 11https://doi.org/10.1074/mcp.O111.016717. O111.016717.

Sennels, L., Bukowski-Wills, J.-C., Rappsilber, J., 2009. Improved results in proteomics by use of local and peptide-class specific false discovery rates. BMC Bioinformatics 10, 179. https://doi.org/10.1186/1471-2105-10-179.

Tang, W.H., Shilov, I.V., Seymour, S.L., 2008. Nonlinear fitting method for determining local false discovery rates from decoy database searches. J. Proteome Res. 7, 3661–3667. https://doi.org/10.1021/pr070492f.

Lambert, J.-P., Ivosev, G., Couzens, A.L., Larsen, B., Taipale, M., Lin, Z.-Y., Zhong, Q., Lindquist, S., Vidal, M., Aebersold, R., Pawson, T., Bonner, R., Tate, S., Gingras, A.-C., 2013. Mapping differential interactomes by affinity purification coupled with data-independent mass spectrometry acquisition. Nat. Methods 10, 1239–1245. https://doi.org/10.1038/nmeth.2702.

Collins, B.C., Gillet, L.C., Rosenberger, G., Röst, H.L., Vichalkovski, A., Gstaiger, M., Aebersold, R., 2013. Quantifying protein interaction dynamics by SWATH mass spectrometry: application to the 14-3-3 system. Nat. Methods 10, 1246–1253. https://doi.org/10.1038/nmeth.2703.

Marques, A.T., Lecchi, C., Grilli, G., Giudice, C., Nodari, S.R., Vinco, L.J., Ceciliani, F., 2016. The effect of transport stress on turkey (Meleagris gallopavo) liver acute phase proteins gene expression. Res. Vet. Sci. 104, 92–95. https://doi.org/10.1016/j.rvsc.2015.11.014.

Bustin, S.A., Benes, V., Garson, J.A., Hellemans, J., Huggett, J., Kubista, M., Mueller, R., Nolan, T., Pfaffl, M.W., Shipley, G.L., Vandesompele, J., Wittwer, C.T., 2009. The MIQE guidelines: minimum information for publication of quantitative real-time PCR experiments. Clin. Chem. 55, 611–622. https://doi.org/10.1373/clinchem.2008.112797.

Thai, M., Graham, N.A., Braas, D., Nehil, M., Komisopoulou, E., Kurdistani, S.K., McCormick, F., Graeber, T.G., Christofk, H.R., 2014. Adenovirus E4ORF1-induced MYC activation promotes host cell anabolic glucose metabolism and virus replication. Cell Metab. 19, 694–701. https://doi.org/10.1016/j.cmet.2014.03.009.

Sanchez, E.L., Lagunoff, M., 2015. Viral activation of cellular metabolism. Virology 479–480, 609–618. https://doi.org/10.1016/j.virol.2015.02.038.

Tchang, V.S.Y., Mekker, A., Siegmund, K., Karrer, U., Pieters, J., 2013. Diverging role for coronin 1 in antiviral CD4+ and CD8+ T cell responses. Mol. Immunol. 56, 683–692. https://doi.org/10.1016/j.molimm.2013.05.003.

Khadivjam, B., Stegen, C., Hogue-Racine, M.-A., El Bilali, N., Döhner, K., Sodeik, B., Lippé, R., 2017. The ATP-Dependent RNA helicase DDX3X modulates herpes simplex virus 1 gene expression. J. Virol. 91. https://doi.org/10.1128/JVI.02411-16.

Adler, K.L., Peng, P.H., Peng, R.K., Klasing, K.C., 2001. The kinetics of hemopexin and alpha1-acid glycoprotein levels induced by injection of inflammatory agents in chickens. Avian Dis. 45, 289–296.

Ceciliani, F., Giordano, A., Spagnolo, V., 2002. The systemic reaction during inflammation: the acute-phase proteins. Protein Pept. Lett. 9, 211–223.

Georgieva, T.M., Koinarski, V.N., Urumova, V.S., Marutsov, P.D., Christov, T.T., Nikolov, J., Chaprazov, T., Walshe, K., Karov, R.S., Georgiev, I.P., Koinarski, Z.V., 2010. Effects of Escherichia coli infection and Eimeria tenella invasion on blood concentrations of some positive acute phase proteins (haptoglobin (PIT 54), fibrinogen and ceruloplasmin) in chickens. Rev. Med. Vet. (Toulouse). 161, 84–89.

Marques, A.T., Nordio, L., Lecchi, C., Grilli, G., Giudice, C., Ceciliani, F., 2017. Widespread extrahepatic expression of acute-phase proteins in healthy chicken (Gallus gallus) tissues. Vet. Immunol. Immunopathol. 190, 10–17. https://doi.org/10.1016/j.vetimm.2017.06.006.

Takagi, T., Naito, Y., Okada, H., Takaoka, M., Oya-Ito, T., Yamada, S., Hirai, Y., Mizushima, K., Yoshida, N., Kamada, K., Katada, K., Uchiyama, K., Ishikawa, T., Handa, O., Yagi, N., Konishi, H., Kokura, S., Ichikawa, H., Yoshikawa, T., 2012. Hemopexin is upregulated in rat intestinal mucosa injured by indomethacin. J. Gastroenterol. Hepatol. 27 (Suppl. 3), 70–75. https://doi.org/10.1111/j.1440-1746.2012.07076.x.

Chen, D., Zheng, J., Gerasimcik, N., Lagerstedt, K., Sjögren, H., Abrahamsson, J., Fogelstrand, L., Mårtensson, I.-L., 2016. The expression pattern of the Pre-B cell receptor components correlates with cellular stage and clinical outcome in acute lymphoblastic leukemia. PLoS One 11, e0162638. https://doi.org/10.1371/journal.pone.0162638.

Bankovich, A.J., Raunser, S., Juo, Z.S., Walz, T., Davis, M.M., Garcia, K.C., 2007. Structural insight into pre-B cell receptor function. Science 316, 291–294. https://doi.org/10.1126/science.1139412.

Maeda, Y., Ohtsuka, H., Tomioka, M., Oikawa, M., 2013. Effect of progesterone on Th1/Th2/Th17 and regulatory T cell-related genes in peripheral blood mononuclear cells during pregnancy in cows. Vet. Res. Commun. 37, 43–49. https://doi.org/10.1007/s11259-012-9545-7.

Frausto, S.D., Lee, E., Tang, H., 2013. Cyclophilins as modulators of viral replication. Viruses 5, 1684–1701. https://doi.org/10.3390/v5071684.

Wang, N., Zhang, L., Chen, Y., Lu, Z., Gao, L., Wang, Y., Gao, Y., Gao, H., Cui, H., Li, K., Liu, C., Zhang, Y., Qi, X., Wang, X., 2015. Cyclophilin a interacts with viral VP4 and inhibits the replication of infectious bursal disease virus. Biomed Res. Int. 2015, 719454. https://doi.org/10.1155/2015/719454.

Dawar, F.U., Tu, J., Khattak, M.N.K., Mei, J., Lin, L., 2017. Cyclophilin a: a key factor in virus replication and potential target for anti-viral therapy. Curr. Issues Mol. Biol. 21, 1–20. https://doi.org/10.21775/cimb.021.001.

Contini, P., Ghio, M., Merlo, A., Poggi, A., Indiveri, F., Puppo, F., 2005. Apoptosis of antigen-specific T lymphocytes upon the engagement of CD8 by soluble HLA class I molecules is Fas ligand/Fas mediated: evidence for the involvement of p56lck, calcium calmodulin kinase II, and Calcium-independent protein kinase C signaling pa. J. Immunol. 175, 7244–7254.

Porat, A., Sagiv, Y., Elazar, Z., 2000. A 56-kDa selenium-binding protein participates in intra-Golgi protein transport. J. Biol. Chem. 275, 14457–14465.

Speckmann, B., Steinbrenner, H., 2014. Selenium and selenoproteins in inflammatory bowel diseases and experimental colitis. Inflamm. Bowel Dis. 20, 1110–1119. https://doi.org/10.1097/MIB.0000000000000020.

Huang, W., Ghisletti, S., Saijo, K., Gandhi, M., Aouadi, M., Tesz, G.J., Zhang, D.X., Yao, J., Czech, M.P., Goode, B.L., Rosenfeld, M.G., Glass, C.K., 2011. Coronin 2A mediates actin-dependent de-repression of inflammatory response genes. Nature 470, 414–418. https://doi.org/10.1038/nature09703.

Nagahara, N., Tanaka, M., Tanaka, Y., Ito, T., 2019. Novel characterization of antioxidant enzyme, 3-Mercaptopyruvate sulfurtransferase-knockout mice: overexpression of the evolutionarily-related enzyme rhodanese. Antioxidants Basel (Basel) 8. https://doi.org/10.3390/antiox8050116.

Gassler, N., Schnölzer, M., Rohr, C., Helmke, B., Kartenbeck, J., Grünewald, S., Laage, R., Schneider, A., Kränzlin, B., Bach, A., Otto, H.F., Autschbach, F., 2002. Expression of calnexin reflects paneth cell differentiation and function. Lab. Invest. 82, 1647–1659.

Huang, Y., Hui, K., Jin, M., Yin, S., Wang, W., Ren, Q., 2016. Two endoplasmic reticulum proteins (calnexin and calreticulin) are involved in innate immunity in Chinese mitten crab (Eriocheir sinensis). Sci. Rep. 6, 27578. https://doi.org/10.1038/srep27578.

Ackerman, M.E., Chalouni, C., Schmidt, M.M., Raman, V.V., Ritter, G., Old, L.J., Mellman, I., Wittrup, K.D., 2008. A33 antigen displays persistent surface expression. Cancer Immunol. Immunother. 57, 1017–1027. https://doi.org/10.1007/s00262-007-0433-x.

Williams, B.B., Tebbutt, N.C., Buchert, M., Putoczki, T.L., Doggett, K., Bao, S., Johnstone, C.N., Masson, F., Hollande, F., Burgess, A.W., Scott, A.M., Ernst, M., Heath, J.K., 2015. Glycoprotein A33 deficiency: a new mouse model of impaired intestinal epithelial barrier function and inflammatory disease. Dis. Model. Mech. 8, 805–815. https://doi.org/10.1242/dmm.019935.